Affleck VS, Coote JH, Pyner S. The projection and synaptic organisation of NTS afferent connections with presympathetic neurons, GABA and nNOS neurons in the paraventricular nucleus of the hypothalamus. 2012, 219, 48-61.

Neuroscience 219 (2012) 48–61

THE PROJECTION AND SYNAPTIC ORGANISATION OF NTS AFFERENT CONNECTIONS WITH PRESYMPATHETIC NEURONS, GABA AND nNOS NEURONS IN THE PARAVENTRICULAR NUCLEUS OF THE HYPOTHALAMUS

V. S. AFFLECK,[a] J. H. COOTE[b] AND S. PYNER[a]*

[a] *School of Biological & Biomedical Sciences, Durham University, Durham DH1 3LE, UK*

[b] *School of Clinical & Experimental Medicine, University of Birmingham, Birmingham B15 2TT, UK*

Abstract—Elevated sympathetic nerve activity, strongly associated with cardiovascular disease, is partly generated from the presympathetic neurons of the paraventricular nucleus of the hypothalamus (PVN). The PVN-presympathetic neurons regulating cardiac and vasomotor sympathetic activity receive information about cardiovascular status from receptors in the heart and circulation. These receptors signal changes via afferent neurons terminating in the nucleus tractus solitarius (NTS), some of which may result in excitation or inhibition of PVN-presympathetic neurons. Understanding the anatomy and neurochemistry of NTS afferent connections within the PVN could provide important clues to the impairment in homeostasis cardiovascular control associated with disease. Transynaptic labelling has shown the presence of neuronal nitric oxide synthase (nNOS)-containing neurons and GABA interneurons that terminate on presympathetic PVN neurons any of which may be the target for NTS afferents. So far NTS connections to these diverse neuronal pools have not been demonstrated and were investigated in this study. Anterograde (biotin dextran amine – BDA) labelling of the ascending projection from the NTS and retrograde (fluorogold – FG or cholera toxin B subunit – CTB) labelling of PVN presympathetic neurons combined with immunohistochemistry for GABA and nNOS was used to identify the terminal neuronal targets of the ascending projection from the NTS. It was shown that NTS afferent terminals are apposed to either PVN-GABA interneurons or to nitric oxide producing neurons or even directly to presympathetic neurons. Furthermore, there was evidence that some NTS axons were positive for vesicular glutamate transporter 2 (vGLUT2). The data provide an anatomical basis for the different functions of cardiovascular receptors that mediate their actions via the NTS–PVN pathways.

Key words: nucleus tractus solitarius, paraventricular nucleus of the hypothalamus, nitric oxide, gamma amino butyric acid, spinally projecting presympathetic neurons.

INTRODUCTION

The paraventricular nucleus of the hypothalamus (PVN) is an important integrating centre for autonomic and neuroendocrine responses to a whole range of stimuli. In particular in conjunction with the rostroventrolateral medulla (RVLM), it plays a critical role in cardiovascular homeostasis (Dampney, 1994; Coote, 2007; Pyner, 2009). The RVLM is primarily concerned with arterial blood pressure regulation and the neural circuitry relating to this control is well documented (Dampney, 1994). The non-endocrine PVN regulates blood pressure in response to stress. This is achieved by activation of a well-characterised pathway, the hypothalamic–pituitary–adrenocortical axis, which promotes the release of adrenocorticotropin hormone from the anterior pituitary (Benarroch, 2005). In addition, blood volume homeostasis is also regulated by this part of the PVN and despite our knowledge of the volume reflex circuit there is still doubt surrounding the precise neural network supporting this function (Hainsworth, 1991; Pyner et al., 2001; Coote, 2005).

It is important to have a thorough knowledge of the afferent and efferent connections and neuronal phenotypes forming the essential neural circuits driving normal sympathetic activation because studies suggest that dysregulation of the sympathetic system is a major contributor to cardiovascular mortality (Grassi et al., 2003; Floras, 2009; Sobotka et al., 2011). In particular, a growing body of evidence indicates that abnormal neurohumoral and sympathetic activation driven by the PVN contributes to various disease conditions including heart failure (HF) and also occurs post myocardial infarction (MI; Floras, 2009). Both an increase in excitation (Zhang et al., 2008) and a decrease in inhibitory mechanisms (Zhang et al., 1997; Li et al., 2002) contribute to the enhanced sympathetic output from the PVN. These conditions are characterised by elevated levels of sympathetic tone to

*Corresponding author. Address: School of Biological & Biomedical Sciences, Durham University, South Road, Durham DH1 3LE, UK. Tel: +44-(0)-191-334-1346; fax: +44-(0)-191-334-1201.
E-mail address: susan.pyner@durham.ac.uk (S. Pyner).

Abbreviations: BDA, biotin dextran amine; CTB, cholera B toxin subunit; DAB, diaminobenzidine; FG, fluorogold; GABA, gamma aminobutyric acid; HF, heart failure; HRP, horseradish peroxidase; IP, intraperitoneal; MI, myocardial infarction; NGS, normal goat serum; NHS, normal horse serum; NO, nitric oxide; nNOS, neuronal nitric oxide synthase; NTS, nucleus tractus solitarius; PB, phosphate buffer; PFA, paraformaldehyde; PVN, paraventricular nucleus of the hypothalamus; RVLM, rostral ventrolateral medulla; SPN, sympathetic preganglionic neurons; TBS, Tris buffered saline; vGLUT2, vesicular glutamate transporter 2.

0306-4522 © 2012 IBRO. Published by Elsevier Ltd. Open access under CC BY-NC-ND license.
http://dx.doi.org/10.1016/j.neuroscience.2012.05.070

cardiac and renal systems with elevated hormonal plasma levels including angiotensin II (Rumantir et al., 1999; Grassi et al., 2003; Floras, 2009).

Presympathetic efferent projections from the PVN target autonomic centres in the brain (RVLM, nucleus tractus solitarius (NTS)) and sympathetic preganglionic neurons (SPN) in the lateral horn of the spinal cord (Hosoya et al., 1991; Pyner and Coote, 1999, 2000). Viral tracing studies using pseudorabies virus or herpes simplex virus have demonstrated the presence of presympathetic neurons in the dorsal cap and lateral parvocellular regions of the PVN. The axons of these neurons project to different end organs and ganglia (Strack et al., 1989a,b; Schramm et al., 1993; Jansen et al., 1995; Huang and Weiss, 1999; Pyner et al., 2001; Watkins et al., 2009). Cardiovascular afferents relaying information about pressure, volume and oxygen saturation terminate mainly within dorsomedial, medial and commissural nuclei of the NTS. The PVN presympathetic neurons in turn receive this cardiovascular information via afferent projections from the NTS (Clement et al., 1972; Karim et al., 1972; Kappagoda et al., 1973; Spyer, 1994). Signals from each of the main groups of cardiovascular receptors that have their first synapse in the NTS have quite different effects on PVN presympathetic neurons. Arterial baroreceptors inhibit (Lovick and Coote, 1988), chemoreceptors excite (Reddy et al., 2005, 2007) and the venous volume receptors inhibit one population and excite another (Lovick and Coote, 1989). Such actions are reflected in the differential responses of the cardiovascular target organs (Coote, 2005).

Connections between the NTS and the PVN have been described in a number of studies (Ricardo and Tongju, 1978; McKellar and Loewy, 1981; Swanson and Sawchenko, 1983; Ter Horst et al., 1989). However, the final neuronal targets for the NTS–PVN afferents are not known. Hence the connections by which the NTS projection to PVN influences the final presympathetic neuronal targets have not been described.

The PVN is surrounded by GABA interneurons that are synaptically connected to dorsal and lateral parvocellular presympathetic neurons. This was shown by transynaptic labelling, using injection of herpes virus into the adrenal medulla (Watkins et al., 2009). In addition, the GABA neurons are surrounded by a subset of neuronal nitric oxide synthase (nNOS)-containing neurons. These are separate from those nNOS-positive neurons within the PVN itself (Watkins et al., 2009). Therefore, it is reasonable to propose that the different actions of NTS afferents may arise from terminations on or close to either parvocellular presympathetic neurons or GABA neurons and nNOS-containing neurons. So far this has not been demonstrated and was investigated in this study. This study has shown NTS ascending afferents target hypothalamic neuronal populations known to regulate sympathetic activity. The NTS afferents terminate on or closely appose: (1) presympathetic and putative magnocellular neurons of the PVN; (2) GABA neurons and (3) nNOS-positive neurons located outside the PVN boundary. Furthermore, there is evidence to suggest glutamate as a neurotransmitter within the NTS afferent projection.

EXPERIMENTAL PROCEDURES

All experiments were approved by the Local Ethics Committee of Durham University and performed in accordance with UK Animals (Scientific Procedures) Act, 1986. Furthermore, all surgical procedures were carried out on anaesthetised animals that minimised suffering with the minimum number of animals used. Animals were killed with an overdose of sodium pentobarbitone (60 mg/kg) at the termination of the experiment.

Injection of anterograde tracer

Twenty-three male Wistar rats (275–315 g) were anaesthetised with intraperitoneal (I.P.) medetomidine 0.25 ml/100 g and ketamine 0.06 ml/100 g. Anterograde labelling methods were similar to those previously described (Pyner and Coote, 1999). After placing the animal in a stereotaxic frame and using stereotaxic co-ordinates (R/C 13.68 mm, L 0.50 mm, D/V 8.00 mm, Paxinos and Watson, 1998; Reiner et al., 2000), 10% biotin dextran amine (BDA, 10 kDa in 10 mM phosphate buffer (PB), pH 7.4) was iontophoresed into the left side of the NTS using a glass micropipette (15–30 μm diameter, $n = 5$) for 20 min (5 μA, DC 7 s on/off, Pyner and Coote, 1999). Alternatively, 10 nl of BDA was pressure injected using a Nanofil syringe ($n = 7$). This combination of injection techniques ensured a small number of ascending afferents from discrete NTS regions could be labelled, as well as a larger number thereby giving the most complete indication of NTS afferent connectivity with the PVN. Only injection sites confined to the regions of the NTS involved in cardiovascular integration (dorsomedial, interstitial, medial and commissural regions) were included for analysis. Injections sited outside of the NTS were excluded and rarely gave projections to the PVN. Injection site distribution is illustrated in Fig. 1D. Following injection, analgesia was administered (0.01 ml/100 g buprenorphine). The animals had *ad libitum* food and water throughout the experimental procedures.

Injection of retrograde tracers

Following recovery (7–10 days) from the NTS injection, animals were re-anaesthetised (as previously described) and either 1 μl of 2% fluorogold (FG) or 2 μl of 0.5% cholera toxin B subunit (CTB, Table 1) was pressure injected into the left side spinal cord intermediolateralis (T2; Watkins et al., 2009). Again, following surgery analgesia (0.01 ml/100 g buprenorphine) was administered. The animals were allowed to survive for a further 7–14 days.

Perfusion

Following the survival period the animals were terminally anaesthetised (sodium pentobarbitone 60 mg/kg). A cannula was then inserted into the descending aorta to allow perfusion with heparinised saline and 4% paraformaldehyde (PFA) or 4% PFA and 0.5% glutaraldehyde in 0.1 M PB (pH 7.4) followed by 10% sucrose-PB. The brain and spinal cord were removed and post fixed overnight at 4 °C before being stored in 30% sucrose-PB (4 °C) until sectioned.

Immunohistochemistry

Immunohistochemistry was carried out on free-floating sections. The sections were cut at 40 μm using a freezing microtome. Every second section underwent immunohistochemistry for the labels of interest, whilst the adjacent sections were counterstained in 1% neutral red. This provided a subset of sections in

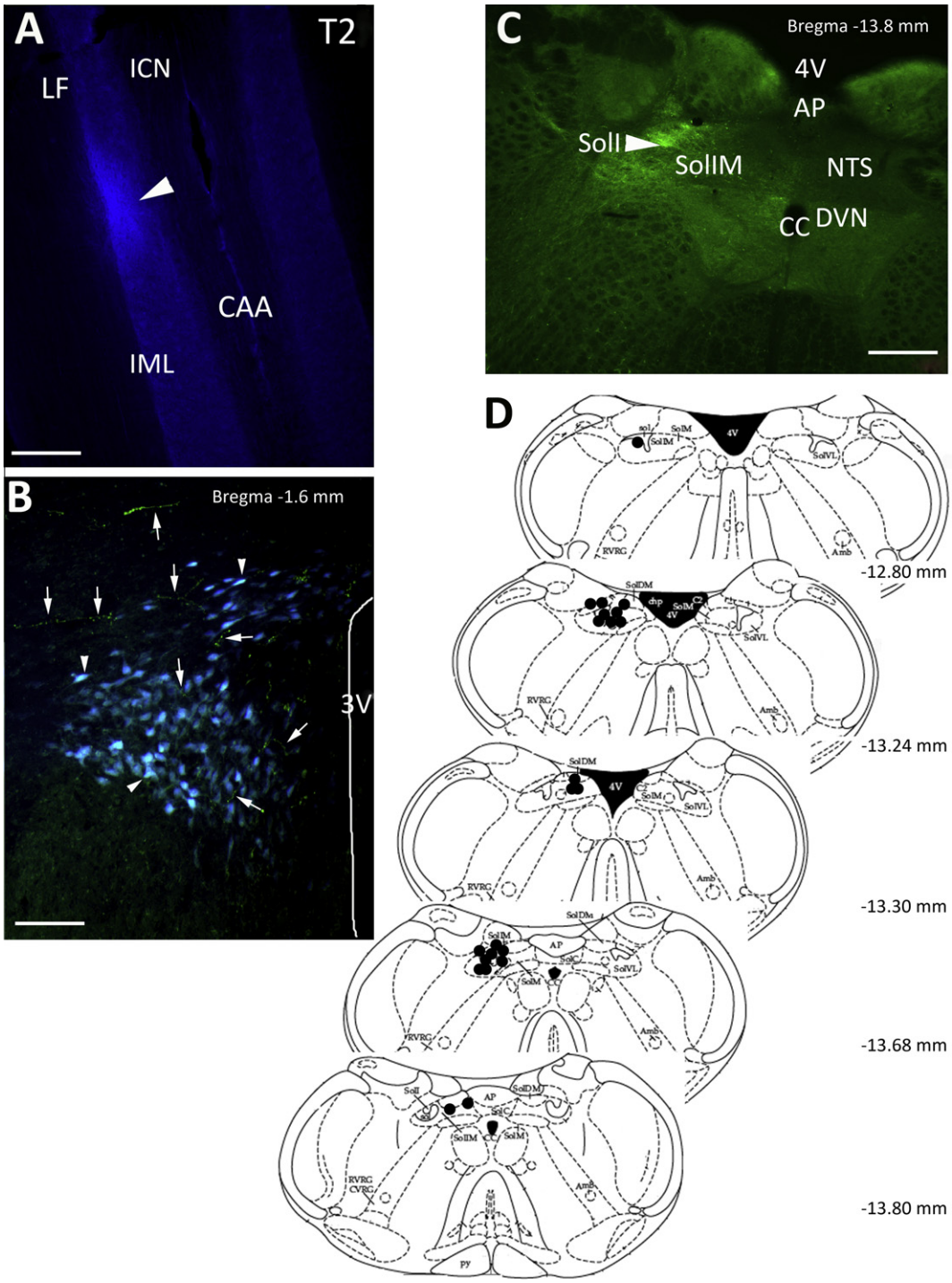

Fig. 1. Spinal cord and NTS injection sites and PVN labelling. (A) Micrograph of a longitudinal section of spinal cord, which shows site of pressure injection of FG (arrowhead) into the IML of the T2 segment that resulted in labelling of neurons in the PVN. (B) Coronal section of the PVN (Bregma −1.6 mm) showing neurons labelled with FG (blue, arrowhead) from the spinal cord and BDA fibres (green, arrows) from the NTS. (C) Micrograph of coronal section of NTS (Bregma −13.8 mm) showing an injection site (arrowhead) of BDA into the interstitial region of the NTS. (D) Coronal map of injection sites into NTS that resulted in axonal labelling in the PVN. Each filled circle represents a deposit of BDA into the NTS that resulted in axonal projections in and around the PVN. *Abbreviations used in the figures:* 3V, 3rd ventricle; 4V, 4th ventricle; Amb, ambiguus nucleus; AP, area postrema; CAA, central autonomic area; CC, central canal; chp, choroid plexus; CVRG, caudo-ventrolateral respiratory group; dp, dorsal parvocellular; DVN, dorsal vagal nucleus; GLU, glutamate; ICN, intercalated nucleus; IML, intermediolateral cell column; LF, lateral funiculus; M, magnocellular; mp, medial parvocellular; NTS, nucleus tractus solitarius; pp, periventricular parvocellular; Py, pyramidal tracts; RVRG, rostral ventral respiratory group; Sol, nucleus of solitary tract; SolC, nucleus of solitary tract, commissural; SolDM, nucleus of solitary tract, dorsomedial; SolI, nucleus of solitary tract interstitial; SolIM, nucleus of solitary tract, intermediate; SolM, nucleus of solitary tract, medial; SolVL, nucleus of solitary tract, ventrolateral; vp, ventral parvocellular. Scale bars A, C = 200 μm; B = 75 μm. (For interpretation of the references to colour in this figure legend, the reader is referred to the web version of this article.)

Table 1. List of immunological reagents, source and concentration

Reagent/antibody	Source/Cat. No.	Concentration	Buffer/pH 7.4
Normal horse serum	Vector Labs –Peterborough, UK S2000	1% or 10%	0.3% Triton X-100-TBS
Normal goat serum	Vector Labs –Peterborough, UK S1000	1% or 10%	0.3% Triton X-100-TBS
Vectastain ABC Kit	Vector Labs –Peterborough, UK PK-6100	As per manufacturer instructions	TBS
ExtrAvidin–HRP	Sigma –Dorset, UK E2886	1:1500	TBS
VIP Peroxidase substrate kit	Vector Labs –Peterborough, UK SK-4600	1:3	TBS
DAB Peroxidase substrate kit	Vector Labs –Peterborough, UK SK-4100	1:3	TBS
Avidin–Biotin blocking kit	Vector Labs –Peterborough, UK SP-2001		TBS
Biotin dextran amine 10K	Molecular Probes –Paisley, UK D1956	10%	10 mM phosphate buffer
Fluorogold	Fluorochrome –Denver, Colorado, USA LLC	2%	0.9% NaCl
Cholera toxin B subunit	List Biologicals –Campbell, California, USA 103B	5%	0.1 M PBS
Guinea pig anti GABA	ABcam –Cambridge, UK ab17413	1:700	1% NGS–0.3% Triton X-100-TBS
Guinea pig anti vGLUT2	Millipore –Oxford, UK MAB5504	1:12,000	1% NGS–0.3% Triton X-100-TBS
Rabbit anti nNOS	Santa Cruz –Santa Cruz, California, USA SC-648	1:400	1% NGS–0.3% Triton X-100-TBS
Goat anti CTB	List Biologicals –Campbell, California, USA 703	1:200,000	1% NHS–0.3% Triton X-100-TBS
Biotinylated donkey anti goat IgG	Jackson Immunoresearch –Suffolk, UK 705-005-1447	1:500	1% NHS–0.3% Triton X-100-TBS
Biotinylated goat anti guinea pig	Jackson Immunoresearch –Suffolk, UK 106-005-003	1:500	1% NGS–0.3% Triton X-100-TBS
Biotinylated goat anti rabbit	Vector Labs–Peterborough, UK BA 1000	1:500	1% NGS–0.3% Triton X-100-TBS
Streptavidin Alexa Fluor 594	Molecular Probes –Paisley, UK S11227	1:200	TBS
Streptavidin Alexa Fluor 488	Molecular Probes –Paisley, UK S11223	1:200	TBS
Streptavidin Alexa Fluor 350	Molecular Probes –Paisley, UK S11249	1:50	TBS
Streptavidin Alexa Fluor 635	Molecular Probes –Paisley, UK S32364	1:200	TBS
Streptavidin Alexa Fluor 555	Molecular Probes –Paisley, UK S21381	1:200	TBS

which the PVN and surrounding neural structures could be easily recognised and used to aid localisation of the same region in the treated sections.

See Table 1 for source and dilution of reagents and antibodies used. All reactions were carried out on a shaker and incubated at room temperature unless otherwise stated.

Biotin dextran amine–cholera toxin B subunit for light microscopy

To reveal BDA, sections were incubated in 10% normal horse serum (NHS)–0.3% Triton-X-100 for 45 min, rinsed in Tris-buffered saline (TBS, 1 × 10 min) then placed in Vectastain ABC reagent made up per manufacturer's instructions for 1 h. Sections were then rinsed in TBS (3 × 10 min) then incubated in Vector VIP substrate (1:3 dilution) for 10 min. Sections were again rinsed in TBS (3 × 10 min, Pyner and Coote, 1999). Prior to CTB visualisation, sections were blocked in avidin–TBS blocking solution (15 min), rinsed in TBS and then blocked with biotin–TBS blocking solution.

Sections were then incubated in 10% NHS–0.3% Triton-X-100 TBS for 30 min, rinsed (3 × 10 min, TBS) then incubated in goat anti CTB made up in 1% NHS–0.3% Triton-X-100-TBS for 2 days. This was followed by 3 × 10 min TBS rinses and incubation in biotinylated donkey anti goat IgG in 1% NHS–0.3% Triton-X-100-TBS for 2 h. The tissue was again rinsed (3 × 10 min, TBS) then incubated in ExtrAvidin–horseradish peroxidase (HRP; 1:1500 dilution in 0.3% Triton-X-100-TBS). The HRP was visualised using the imidazole-intensified diaminobenzidine (DAB) reaction using glucose oxidase to generate hydrogen peroxide (Llewellyn-Smith et al., 2005). Briefly, sections were incubated in a mixture of imidazole-intensified-DAB (100 mM Tris–HCl, pH 7.6, 1 M imidazole w/v, 0.4% ammonium chloride, 20% D-glucose, 0.05% sodium azide w/v, 10 mg DAB). After 10 min, fresh mixture with the addition of glucose oxidase (1 μl/ml) was added and the reaction proceeded until brown neurons were visible. The reaction was stopped using large volumes of TBS, with final rinses in TBS and distilled water. Sections were mounted onto gelatinised slides and air-dried. The sections were dehydrated through a graded series of alcohols, cleared in xylene and a coverslip positioned using DPX mounting medium.

Biotin dextran amine–cholera toxin B subunit for epifluorescence

BDA sections were incubated in 10% NHS–0.3% Triton-X-100 for 45 min, rinsed in Tris-buffered saline (TBS, 1 × 10 min) and then incubated in an appropriate streptavidin Alexa Fluor 594 or 488 for 2 h. The sections then had a further rinse in TBS followed by avidin–biotin blocking and incubation in goat anti CTB with streptavidin Alexa Fluor 594 or 488 (Watkins et al., 2009).

GABA, nNOS and vesicular glutamate transporter 2 (vGLUT2) combined with BDA–CTB for epifluorescence

The relationship between BDA–CTB and various neurotransmitters was investigated by taking the BDA–CTB processed tissue, carrying out a further avidin–biotin blocking step then incubating in the appropriate combination of primary antibodies (guinea pig anti GABA, guinea pig anti vGLUT2 and rabbit anti nNOS). The sections were incubated in 10% normal goat serum (NGS)–0.3% Triton-X-100-TBS for 30 min followed by 3 × 10 min rinses and then incubated in the primary antibody made up in 1% NGS–

0.3% Triton-X-100-TBS for 2 days for GABA and vGLUT2 and 1 day for nNOS. This was followed by TBS rinsing (3 × 10 min) and the addition of biotinylated goat anti guinea pig or rabbit IgG for 2 h. After further TBS rinses (3 × 10 min) the tissue was incubated in a suitable fluorochrome, e.g. streptavidin Alexa Fluor 350, 488, 555 or 594 (Watkins et al., 2009).

Image acquisition, visualisation and analysis

Sections were examined using a Zeiss Axioskop 2 under bright field or epifluorescence illumination for the existence of putative connections between the NTS and GABAergic interneurons, nNOS-containing neurons and presympathetic neurons of the PVN. Digital images were captured with Hamamatsu Orca 285 CCD or Micropublisher 3.3 RTV cameras controlled by Improvision Volocity (Acquisition, Restoration and Visualisation) software (v. 6.0). Using epifluorescence illumination, images were obtained by capturing a series of z-stacks sampled at 0.2 μm using standard wide field fluorescence. The acquired 3D volume was deconvolved using iterative restoration and the appropriate point spread function (PSF). The PSF models the behaviour of light in the optical system and used the same parameters under which the data for deconvolution were acquired. In this instance PSF were calculated for each objective using the Volocity specified parameters of widefield, numerical aperture, medium refractive index and emission wavelength. This process reassigned out-of-focus haze without subtracting it from the data to improve resolution in the *X*, *Y* and significantly *Z* planes. This produced a confocal-like quality image. The most appropriate single *Z* plane image was then converted to 3-D Opacity image, which is a high-resolution render with options to display data in different views. Images were displayed as isosurface views selected from their respective 3D Opacity image. Isosurface is a form of indirect rendering, which identifies a surface around objects where all voxel intensity values are the same. Isosurface rendering generates a 3D non-transparent solid of the surface elements. This image manipulation further improves clarity to aid in identifying possible sites of synaptic contact and transmitter co-localisation (Wouterlood et al., 2002, 2003; Henny and Jones, 2006; Feng et al., 2007).

The final images were imported into Adobe Photoshop (CS4 extended v. 11.02), which was used to adjust brightness and contrast. Processed images were grouped into plates and labelled in Adobe Photoshop. For cell counting, six coronal sections at the same rostro-caudal level (Bregma −1.60 to −2.12 mm, Paxinos and Watson, 1998) of the PVN were examined. Cell counts are expressed as mean ± SEM. No correction for double counting was made and neurons were counted in those sections where a nucleus was evident.

Antibody specificity

Control sections were incubated in TBS with the omission of primary or secondary antibodies. With this regime no staining was observed. In further controls, sections were also incubated with

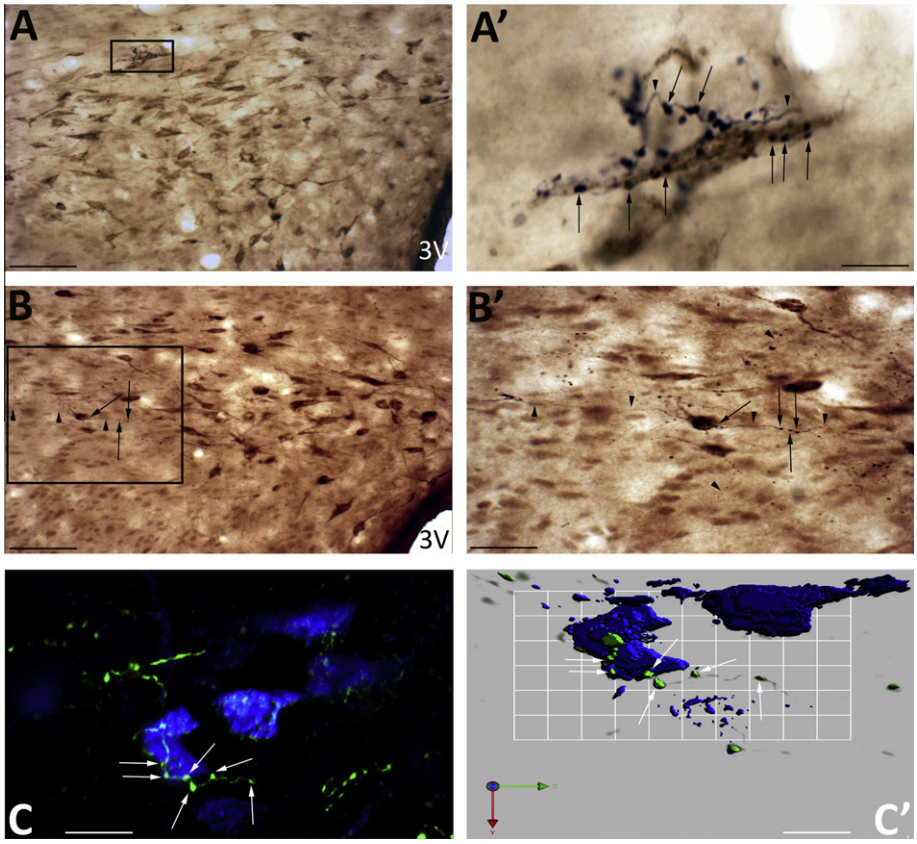

Fig. 2. Spinally projecting neurons as targets for axons projecting from the NTS. Views of the dorsal cap region of PVN showing NTS axons (black) with close appositions to the cell bodies (A, A′) and dendrites (B, B′) of the cholera toxin-labelled spinally projecting presympathetic neurons (brown). (A′) Multiple axons (arrowhead) wound around cells where synaptic boutons (arrow) apposed the cell soma. Similarly, axons (B′) can be observed to traverse cell bodies in their passage through the PVN. These axons had numerous boutons (arrow) interspersed by non-bouton regions (arrowhead). (C) A deconvolved image showing the course of an axon (green) as it crossed the cell soma of a FG-labelled presympathetic neuron (blue) with multi bouton appositions over the cell soma (arrow). (C′) An isosurface 3-D rendered view of (C) revealing the close association between the green NTS boutons (arrows) with the preautonomic neurons (blue). Scale bars A, B = 60 μm; A′ = 6 μm; B′ = 30 μm; C = 15 μm; C′ = 8 μm. (For interpretation of the references to colour in this figure legend, the reader is referred to the web version of this article.)

the primary antibodies, which had been previously preabsorbed with their respective blocking peptides. Again no staining was evident.

For application of a second biotinylated secondary antibody during double labelling experiments, an avidin–biotin blocking step was employed prior to application of the primary antibody of the second target of interest. This pre-treatment of avidin followed by biotin blocked any remaining biotin binding sites. Controls to ensure lack of chromogen cross over staining involved incubation of sections with the omission of avidin or biotin or both. Only after incubation in avidin followed by biotin was cross over staining avoided.

RESULTS

Spinal cord and NTS injection sites

FG (five rats) or CTB (seven rats) injected into the area encompassing the lateral horn of the T2 thoracic spinal cord spread into the lateral funiculus and intercalated region (Fig. 1A). Following the injections, into the 12 animals, labelled presympathetic neurons were observed in the PVN, most predominately in the ventral and dorsal regions (Fig. 1B). Labelled neurons were also present in the ventral medulla but these were not investigated further.

In the same 12 rats, BDA injected at different rostro-caudal levels encompassing the dorsomedial, interstitial, medial and commissural regions of the NTS (Fig. 1C, D) resulted in axonal projections that could be observed to course within and around the PVN (Figs. 1B, 2B, 4C). There was no difference in terminal projection target from either iontophoresis or pressure injection protocols. A greater fibre density in and around the PVN was noticed following pressure injection. Injection sites found to lie outside the above regions of the NTS, rarely gave rise to ascending axons directed towards the PVN but appeared to project within the medulla and were not traced further.

Distribution of PVN presympathetic (spinally projecting) neurons

The retrograde tracer FG was confined to the soma cytoplasm and proximal dendritic region of the neurons in the PVN (Fig. 1B), while CTB was not only present in the soma cytoplasm but extended further to reveal more of the dendritic arborisation (Fig. 2A, A′, B, B′).

In five rats FG labelled 390 ± 69 and in a further seven rats CTB labelled 317 ± 55 spinally projecting presympathetic neurons on the side of the PVN ipsilateral to the injection. This gave a mean of 347 ± 42 (n = 12, range 136–585) presympathetic neurons that were scattered throughout the ipsilateral and rostro-caudal extent of the parvocellular subdivisions of the PVN. In particular presympathetic neurons were mainly localised to the lateral and medial subdivisions and the dorsal cap region of

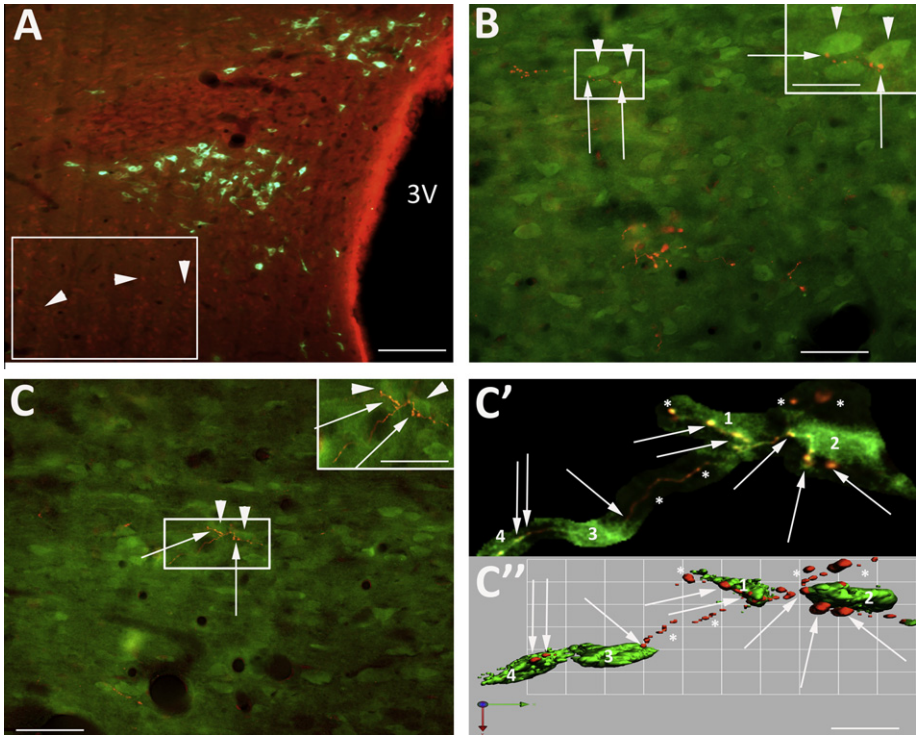

Fig. 3. NTS originating axons course through the GABA neuronal pools adjacent to the PVN. (A) Coronal section at Bregma −1.88 mm showing the PVN-containing spinally projecting neurons (green) and GABA interneurons (box, arrowheads). (B, C) Examples of orange NTS axons coursing through the GABA neuronal pools (green, arrowhead) that had synaptic boutons (arrow) closely apposed to the cell bodies of the GABA neurons (boxed insert right hand corner B, C). (C′) deconvolved image of boxed area in (C). The course of the orange axon (asterisk) can be traced crossing the green GABA-positive cells (1–4). The arrows indicate the sites of en passent boutons across the cells. (C″) Isosurface 3-D rendered image of (C′), which provides evidence in support that axons (asterisk) with en passent boutons (arrows) could be in synaptic contact with the GABA-positive neurons 1–4. Scale bars A = 120 μm; B = 13 μm and 6 μm; C = 14 μm and 8 μm; C = 15 μm and 8 μm; C′, C″ = 5 μm. (For interpretation of the references to colour in this figure legend, the reader is referred to the web version of this article.)

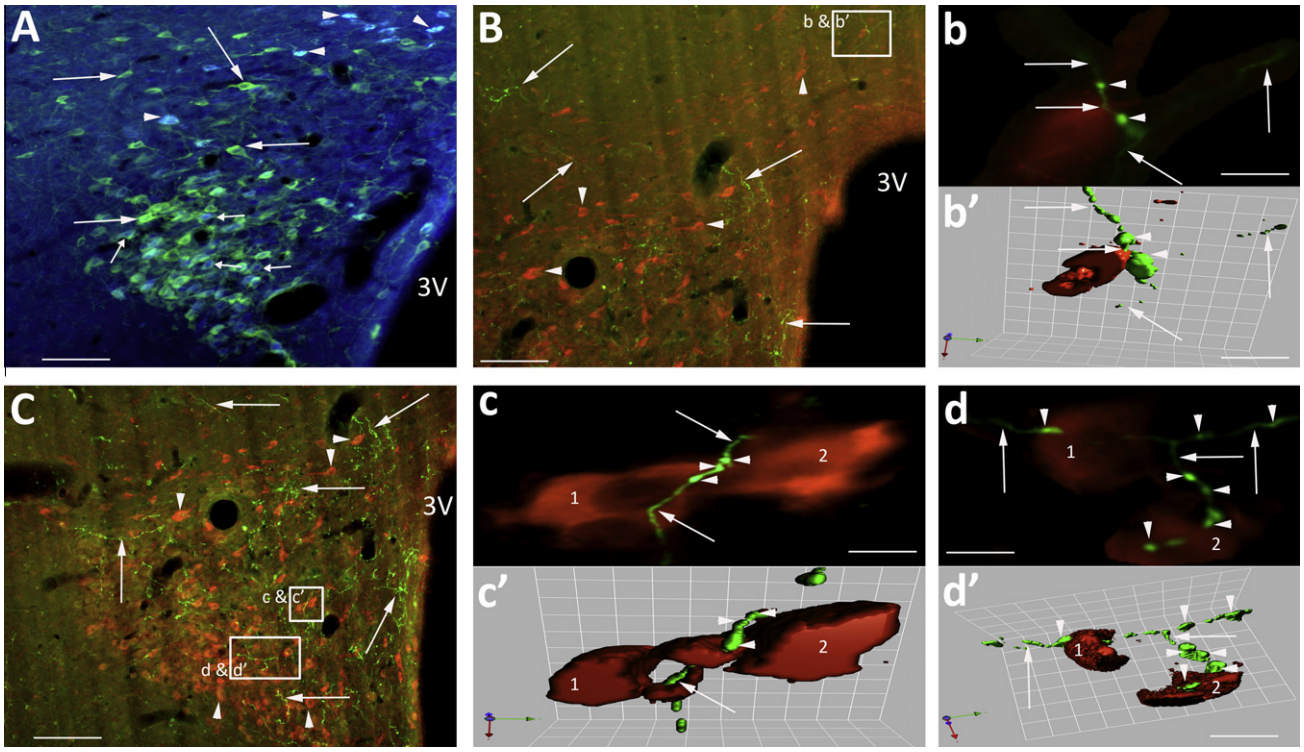

Fig. 4. nNOS-positive neurons within and adjacent to the PVN associated with NTS axons. (A) Coronal section (Bregma −2.12 mm) showing PVN with presympathetic neurons (blue, arrowhead) and intermingled nNOS-positive neurons (green, arrows) that lie within the PVN. The small arrows indicate presympathetic neurons that are also positive for nNOS. (B, C) NTS axons (green, arrows) intermingled with nNOS-positive neurons (orange, arrowheads) in the more ventrolateral magnocellular region, as well as in the parvocellular region of PVN and adjacent to the PVN. (b) Deconvolved images of boxed area in (B). An NTS axon (arrows) crossed the nNOS-positive neuron outside the nominal boundary of the PVN where two boutons (arrowhead) were closely apposed to the cell body. (b′) isosurface 3-D rendered image of (b) highlighting the close bouton association (arrowhead) with the nNOS cell body. The arrows indicate axons passing close by as determined from image (b). (c, c′, d, d′) Deconvolved and isosurface 3-D rendered images from (C) of NTS axonal (arrows) relationship with nNOS neurons. Numerous boutons (arrowhead) were adjacent to the cell bodies. Apparent hole in (c′) is the position of the cell nucleus that does not stain for nNOS so appears empty when viewed as an isosurface structure. Scale bars A = 60 μm; B, C = 120 μm; b = 7 μm; b′ = 9 μm; c, c′ = 8 μm; d = 7 μm, d′ = 9 μm. (For interpretation of the references to colour in this figure legend, the reader is referred to the web version of this article.)

PVN (Figs. 1B, 2A, B, 3A, 5A). A small number of FG presympathetic neurons (128 ± 19.5, n = 12) were also observed in the parvocellular nuclei of the contralateral PVN.

NTS relationship with PVN presympathetic neurons

The anterograde tracer BDA deposited in the NTS (Fig. 1D) resulted in the presence of ipsilateral-ascending axons coursing around and into the PVN with varicose terminals and boutons close to neurons in these regions (Fig. 2A′, B′). The varicosities along the axons were oval in shape or were found at the end of short terminal branches. The axons entered the PVN at its lateral and dorsal boundaries (Fig. 1B). Those axons passing close to neurons were characterised by the presence of en passent boutons (Fig. 2A′, B′, C, C′).

Many of the varicosities of the NTS terminal axons in the PVN appeared to be in close contact with soma and dendrites of CTB or FG-labelled presympathetic neurons (Fig. 2A–C′). These NTS varicose axons were also observed to traverse numerous cell bodies making multi-en passent bouton contacts on their passage to the PVN (Fig. 2B′). This is best illustrated in the deconvolved image of an axon crossing the soma of a FG-labelled presympathetic neuron illustrated in Fig. 2C, C′.

NTS fibres and GABA neurons

Neurons immunopositive for GABA were found above the dorsal cap region of the PVN and lateral and ventral (Fig. 3A) to the nucleus in similar locations to those we have previously described (Watkins et al., 2009). BDA-labelled fibres from NTS with en passent boutons coursed amongst the GABA neurons as the axons projected towards the PVN (Fig. 3B, C). These en passent varicosities lay so close to the cell bodies of the GABA neurons (Fig. 3C′, C″) that they gave the appearance of being apposed to the cell soma and dendrites. This is illustrated in Fig. 3C where a high power deconvolved image (Fig. 3C′) of the boxed area reveals an orange NTS axon (asterisk) that can be traced crossing green GABA-immunoreactive (IR) neurons making close appositions at several sites. The possibility that these sites are en passent synapses is supported by the closeness of the varicosities (red) to three GABA neurons revealed in the isosurface 3-D rendered image of this same region (Fig. 3C″).

NTS axons and nNOS neurons

nNOS immunoreactive neurons were observed within the PVN (Fig. 4A). There were three clearly identified nNOS-

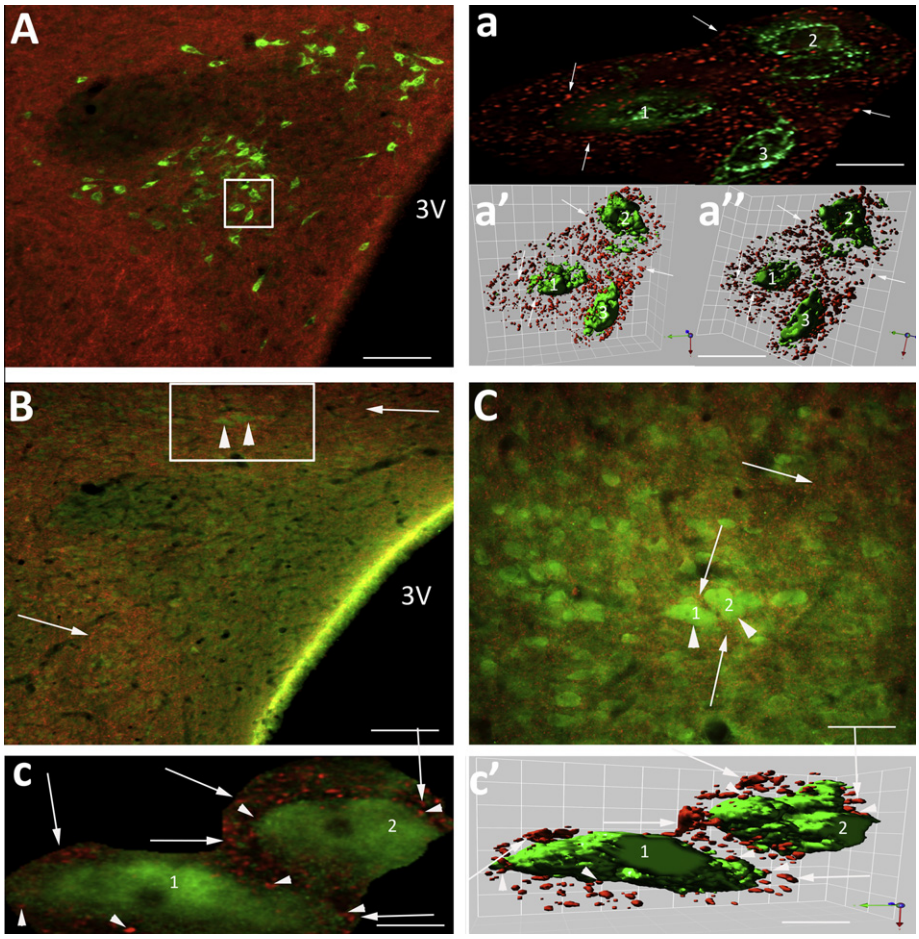

Fig. 5. Relationship between spinally projecting, GABA neurons and vGLUT2 transporter. (A) Micrograph at Bregma −1.80 mm showing PVN with CTB-labelled presympathetic neurons (green) surrounded by varicosities stained positive for the vGLUT2 transporter (red). (a) Deconvolved image of boxed area in (A). The three presympathetic neurons (1–3) were surrounded by vGLUT2-positive varicosities (arrows). (a′, a″) Isosurface 3-D rendered views suggest some varicosities may be closely associated with the neuronal cell surface but the majority display no relationship with the presympathetic neurons. (B) Coronal section with the PVN defined by orange boutons labelled for vGLUT2 transporter (arrow) passing through GABA interneurons (boxed area, arrowhead). (C) High power of boxed area in (B) illustrating the relationship between two GABA interneurons (arrowhead) and vGLUT2 varicosities (arrows). (c, c′) Deconvolved and isosurface 3-D rendered images to show that the majority of vGLUT2-positive boutons (arrow) surround the GABA interneurons while a small number are closely apposed (arrowhead). Scale bars A, B = 60 μm; a, a″ = 11 μm; C = 11 μm; c, c′ = 5 μm. (For interpretation of the references to colour in this figure legend, the reader is referred to the web version of this article.)

positive populations of neurons. The main group lay in the magnocellular subdivision of the PVN, shown by the orange/red neurons located in the ventral part of the PVN (Fig. 4B, C), and comprised 586 ± 58, (ipsilateral to injection site, $n = 3$) nNOS-IR-positive neurons. A second group of nNOS-IR neurons was located in the parvocellular subdivisions where ipsilaterally a small percentage of presympathetic CTB-labelled neurons displayed nNOS immunoreactivity (8.7 ± 3.7%, $n = 3$; Fig. 4A), confirmed by higher power deconvolved image (not shown). A third group of nNOS-positive neurons was present at the PVN boundaries, close by the GABA interneurons, confirming our previous description (Watkins et al., 2009). It was apparent that in all the three nNOS-IR areas the axon terminal projections from the NTS had a widespread distribution of en passent appositions on more than one population of neurons within the PVN and the immediate surroundings. Examples of which are shown in Fig. 4b, b′, c, c′, d, d′.

Glutamate transporter vGLUT2-labelled nerve terminals

In three rats, sections were incubated in anti vGLUT2 in addition to processing for GABA, nNOS, BDA or CTB. Axons that stained positive for vGLUT2 transporter formed a dense network surrounding the PVN (Figs. 5 and 6) as well as encroaching within its boundaries to intermingle with the spinally projecting neurons (Fig. 5A). In Fig. 5a the deconvolved image of the box region (Fig. 5A) reveals three presympathetic CTB-labelled neurons (1–3) surrounded by vGLUT2-IR terminals (red spots). Isosurface 3-D rendered views reveal the vGLUT2 en passant boutons apposed to the soma of the presympathetic neuron (Fig. 5a′, a″). A similar pattern of vGLUT2 transporter labelling was observed in relation to the GABA (Fig. 5B, C, c, c′) and nNOS populations (Fig. 6A, a, a″).

In contrast to this general distribution of vGLUT2-positive terminals only a small number of the vGLUT2-IR

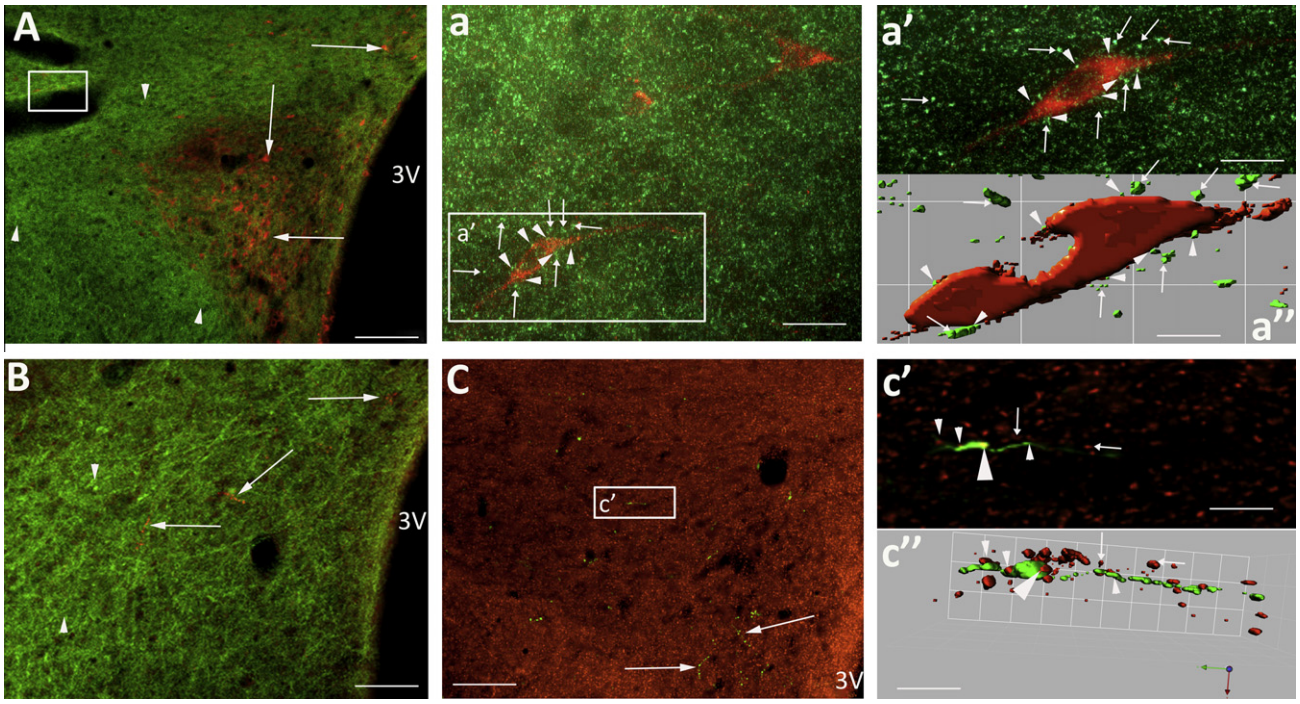

Fig. 6. Relationship between nNOS neurons, NTS axons and vGLUT2 transporter. (A) Low power micrograph showing vGLUT2 transporter-IR-labelled varicosities (green, arrowhead) surrounding nNOS-IR-positive neurons (orange, arrows). (a) Boxed area (a′) from (A) showing the widespread dense distribution of vGLUT2-positive varicosities relative to an nNOS neuron. The arrows indicate varicosities not associated with the neuron (majority) and those closely apposed (arrowhead). (a′, a″) Deconvolved and isosurface images of nNOS neuron (boxed area a) surrounded by vGLUT2. The arrowheads highlight appositions and arrows indicate non-apposed boutons. (B, C) Relationship between NTS axons (arrows) and vGLUT2 transporter varicosities (arrowhead). (c′, c″) Deconvolved and isosurface 3D-rendered image from box in (C). This shows vGLUT2 transporter co-localised with an NTS bouton (yellow, big arrowhead). A number of vGLUT2 boutons are in close relationship with the NTS axon (small arrowhead). The arrows indicate boutons some distance from this particular axon. Scale bars A–C = 60 μm; a = 20 μm; a′ = 15 μm; a″ = 5 μm; c′ = 6 μm; c″ = 5 μm. (For interpretation of the references to colour in this figure legend, the reader is referred to the web version of this article.)

axons within the PVN were BDA-labelled NTS projections (Fig. 7). In a count of 332 BDA-labelled boutons (n = 3 rats) 28 appeared to be positive for vGLUT equating to 1.3 ± 0.3%.

DISCUSSION

This study provides the first evidence that ascending axonal fibres from the NTS that were labelled with BDA specifically target four types of PVN-associated neurons: presympathetic and putative magnocellular (nNOS) lying within the nucleus with GABA and nNOS positive surrounding the PVN (Fig. 8). Furthermore, we have shown the glutamate transporter vGLUT2 to be co-localised with a small number of the boutons of the BDA-labelled axons suggesting glutamate to be a transmitter candidate for this pathway. The observation of these connections completes the link between sensory inputs to the NTS and specific neural targets in the PVN that either directly or indirectly regulate sympathetic nerve activity. Since the main cardiovascular receptors, baroreceptors, chemoreceptors and atrial receptors terminate in the region of the NTS where the BDA-labelled axons originated it is tempting to suggest that the connections in the PVN are representative of the reflex pathway of each of these receptors.

NTS-ascending axonal relationship with presympathetic neurons

A number of studies report reciprocal connections between the NTS and PVN (McKellar and Loewy, 1981; Swanson and Sawchenko, 1983; Kannan and Yamashita, 1988). Importantly, these studies reveal the NTS to have terminal axons in the region of the PVN involved with cardiovascular homeostasis (Ricardo and Tongju, 1978; McKellar and Loewy, 1981; Swanson and Sawchenko, 1983; Ter Horst et al., 1989). However, until now the final neuronal targets for the ascending NTS–PVN projection were not known. We have identified at least four targets: presympathetic and putative magnocellular (nNOS) neurons in the PVN and GABA and nNOS positive surrounding the PVN. We have specifically demonstrated numerous sites where the NTS en passent axonal boutons are closely apposed to spinally projecting presympathetic neuronal soma and dendrites. The close apposition of the NTS varicose axon indicated multiple points of possible synaptic contact with the cell soma and dendrites of the presympathetic PVN neurons, albeit at the resolution of light and epifluorescence microscopy. A further arrangement was also seen, whereby the en passent boutons were close to neuronal target structures but were not in apparent direct contact. Previous studies (Wouterlood

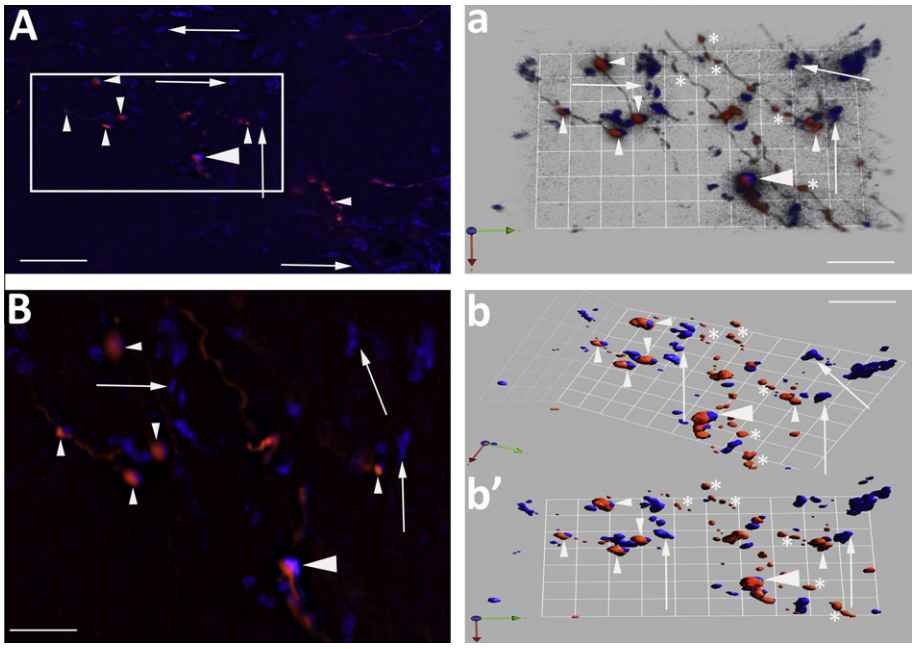

Fig. 7. NTS axonal boutons and expression of the vGLUT2 transporter. (A) NTS axonal boutons (red) within the PVN that express vGLUT2 (blue). The boxed area is expanded in (B). The large arrowhead (A, B, a, b, b′) indicates a possible co-localised axonal bouton while the small arrowheads show NTS (red) only and arrows vGLUT2 (blue) boutons only. (a) Combines a deconvolved and isosurface 3-D rendered view to reveal the relationship between NTS and vGLUT2 expression. Numerous NTS and vGLUT2 boutons are apposed (small arrowheads). A proportion of NTS (asterisk) and vGLUT2 (arrows) boutons show no relationship. The large arrowhead indicates a possible co-localisation of vGLUT2 and NTS axon. (b′, b″) Isosurface 3-D rendered images presented in different planes indicating an NTS bouton that could be expressing vGLUT2 (large arrowhead). The small arrowheads indicate sites where NTS boutons and vGLUT2 transporter are closely associated. However, the majority of vGLUT2 (arrows) and NTS axons (asterisk) are not associated. Scale bars A = 15 μm; B = 10 μm; a = 14 μm; b′ = 10 μm. (For interpretation of the references to colour in this figure legend, the reader is referred to the web version of this article.)

et al., 2002, 2003; Henny and Jones, 2006) have used 3D-isoform rendering to confirm direct synaptic contact from fluorescent-deconvolved images. The rendered images were used to view the structures of interest (bouton/cell body) from varying angles and magnifications. From this approach the absence of space between structures from any angle could be observed. In addition, these authors also identified post-synaptic scaffolding proteins as markers of the synaptic junctions. Our images when viewed as isosurface rendered structures revealed absence and presence of space between the axonal bouton and cell body. We cannot conclusively state the rendered images provide evidence of direct synaptic contact, as we did not stain for post-synaptic scaffolding proteins. However, the nature of the rendered images provides strong evidence towards the NTS–PVN terminal axons being synaptically and non-synaptically connected to the neuronal targets.

In addition to the evidence for apposition provided by isoform rendering there are other robust arguments that strongly support our interpretation of the data as evidence of direct synaptic connectivity without electron microscopic confirmation of synaptic specialisation (Pilowsky et al., 1992). Pilowsky and colleagues suggested that at the light microscopic level the type of close relationship we observe is usually indicative of the presence of a synaptic contact. In their study comparing light and electron microscope images of substance P immunoreactive boutons on SPN, they found that close apposition indicated that there is an even chance that a real synapse is present (Pilowsky et al., 1992). Also, without synaptic specialisations close appositions can indicate the possibility for remote release of peptide having a functional influence by modulation of the neuronal target (Jan and Jan, 1985). This would be especially relevant if catecholamines are a transmitter candidate in this pathway (see below). Remote release of monoamines has been reported as a method of neuronal modulation (Fuxe et al., 2010).

NTS axonal relationship with GABAergic and nitrergic immunopositive neurons

A similar NTS axonal en passent bouton relationship was observed for both GABA and nNOS immunopositive neurons. The varicosities of NTS terminal axons as they coursed towards the PVN, made close appositions to the cell soma of GABAergic neurons located at the outer anatomical border of the PVN. We have previously shown that these GABA neurons are synaptically connected to a population of presympathetic neurons that influence adrenal medullary function and it is likely that it is the same for other presympathetic neurons (Watkins et al., 2009).

In regard to nNOS neurons, within the PVN there are a small number of presympathetic neurons that express nNOS and NTS terminal varicosities were observed to be sufficiently close to indicate appositions or even to make contact to their soma to suggest a true synaptic relationship. This could reflect the pathway of a specific peripheral receptor input to NTS, which then projects directly to excite a specific population of PVN

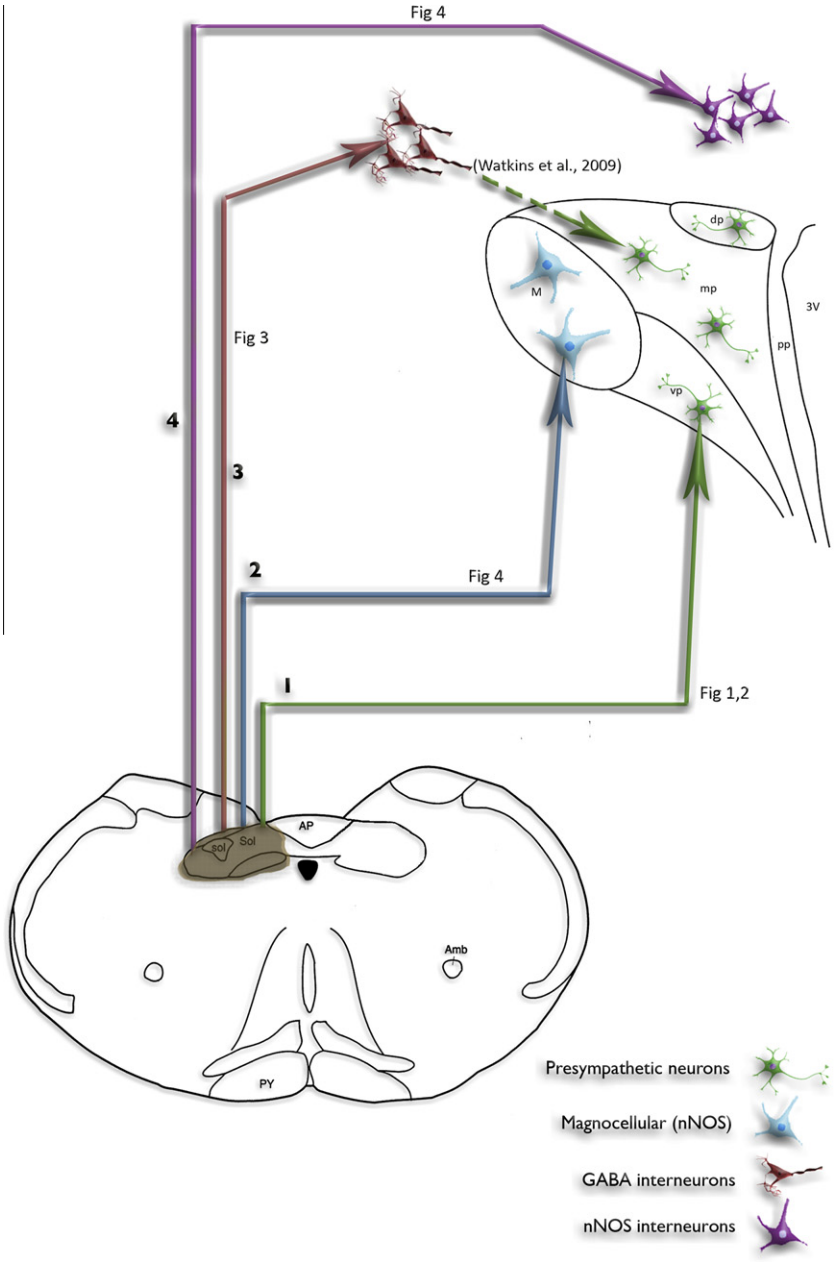

Fig. 8. Drawing summarising the four main axonal pathways projecting from the NTS to the PVN and surrounding region. Ascending NTS axons project to at least four neuronal targets in and around the PVN that are associated with cardiovascular control: (1) Projections to the spinally projecting neurons (green) within the parvocellular regions of the PVN. (2) Projections to the nNOS-containing magnocellular neurons (blue) of the PVN. (3) Projections to the GABA interneurons (red) surrounding the PVN, which are in synaptic contact (Watkins et al., 2009) with spinally projecting neurons. (4) Projections to the nNOS-containing interneurons (pink) that border the PVN (Watkins et al., 2009). The release of NO from these neurons could affect GABA interneurons and/or spinally projecting neurons. (For interpretation of the references to colour in this figure legend, the reader is referred to the web version of this article.)

presympathetic neurons. A second group of nNOS neurons lie in the magnocellular region of the PVN and are a major cellular source of nitric oxide (NO) in the PVN (Nylén et al., 2001; Stern, 2004). These again were surrounded by NTS-originating axons that were in close apposition or synaptic contact. There is evidence that NO released from magnocellular neurons has a modulatory effect on the activity of parvocellular presympathetic neurons by extracellular diffusion (Stern, 2004). Here we have provided evidence for a possible role for the NTS in the release of NO from the magnocellular neurons to modulate presympathetic activity possibly in relation to a cardiovascular stimulus.

A third population of nNOS-containing neurons were identified outside the PVN boundary. Again these were shown to have NTS axons closely intermingled with cell soma revealing a further network by which the NTS could influence presympathetic activity using nNOS as an inter-

mediary. The target for the released NO from this population is not known, however the gas could diffuse to modulate the GABA neurons and presympathetic neurons.

NTS-ascending axons are glutamatergic

An important question answered in part by this study is that of the neurochemical nature of the synaptic boutons of some of the NTS-ascending afferent fibres to the PVN. These may be associated with presympathetic and GABA neurons and nNOS-positive neurons. Using an antibody to vGLUT2 transporter we provided evidence of co-localisation of this transporter with boutons in a limited number of the BDA-labelled NTS originating fibres. This suggests that glutamate is a transmitter candidate released by these terminals although it does not rule out that other transmitters are co-released (Herzog et al., 2001; Lin et al., 2003). Since only a few NTS-BDA-labelled axons terminating in or around the PVN showed immunoreactivity to vGLUT2 it would appear that ascending afferents from NTS utilise agents other than glutamate raising the possibility that some could even be directly inhibitory to PVN cells. While many different neurotransmitters have been identified in the NTS complex (Maley, 1996), there is no evidence so far, to suggest neurons containing any of these, project to the PVN. There is however evidence relating to the noradrenaline-containing cells of the A2 group lying in or around the NTS (Sawchenko and Swanson, 1982; Duale et al., 2007). Noradrenaline terminals elsewhere can be inhibitory or excitatory depending upon the associated postsynaptic receptor. For example in the spinal cord alpha 1 adrenoreceptors are excitatory and alpha 2 adrenoreceptors are inhibitory (Inokuchi et al., 1992).

Nonetheless it is clear that glutamate may play an important excitatory role in the actions of a few NTS afferents terminating in or close to PVN. A recent publication supports our observation of a limited glutamatergic NTS-ascending projection to the PVN (Ziegler et al., 2012). Using *in situ* hybridisation for vGLUT2 transporter these authors demonstrated relatively few NTS-ascending axons projecting to the PVN were vGLUT2-positive while other brain regions such as the periaqueductal grey had a substantial PVN projection that was vGLUT2-positive.

Excitatory glutamatergic inputs to the PVN have been described from other hypothalamic nuclei as well as thalamic and amygdala brain regions (Boudaba et al., 1996; Li et al., 2004; Li and Pan, 2006, 2007; Ulrich-Lai et al., 2011). In accord with this, the activation of PVN presympathetic neurons by intracarotid hyperosmotic solutions is blocked by the non-selective ionotropic receptor antagonist kynurenic acid microinjected into the PVN (Antunes et al., 2006; Yang and Coote, 2006).

Functional considerations

The co-ordinated activity of distinct neuronal populations within the PVN contributes to cardiovascular homeostasis. For example, renal and cardiac presympathetic PVN neurons are involved in the moment-by-moment control of plasma volume homeostasis (Coote, 2005), which is partly maintained by the atrial volume reflex arc (Hainsworth, 1991; Pyner et al., 2002; Yang and Coote, 2003, 2006). Mechanoreceptors located at the venous atrial junction of the heart signal plasma volume status to the NTS. Stimulation of these receptors can cause a reflex inhibition of renal sympathetic activity and a simultaneous inhibition of cardiac sympathetic activity. Therefore, renal and cardiac presympathetic PVN neurons are likely to be dependent on the connections from the NTS, demonstrated in the present study. Thus the NTS axons projecting directly to appose some PVN presympathetic neurons could represent an excitatory arm of the atrial receptor reflex, whilst those projecting to GABA neurons or nNOS-positive neurons may be an inhibitory arm of the reflex. This accords with the evidence showing that plasma volume expansion excites some PVN neurons and inhibits others (Lovick and Coote, 1988). We tentatively interpret these observations as the first anatomical evidence that may possibly represent a central afferent pathway of a reflex that has a differential action on sympathetic outflow.

Similarly the inhibition of presympathetic neurons caused by stimulation of arterial baroreceptors could be dependent on the NTS connections we observed with the GABA neurons surrounding the PVN. Additionally, it is tempting to speculate that the excitation elicited by arterial chemoreceptor activation is mediated by the NTS axons that appear to directly appose PVN presympathetic neurons.

Numerous studies have demonstrated the importance of the atrial receptor reflex and the pivotal role of the PVN for normal blood plasma volume regulation (Lovick et al., 1993; Haselton et al., 1994; Coote, 2005) but in addition there is a growing consensus for an impairment of this reflex in cardiovascular disorders such as hypertension (Goto et al., 1981; Ciriello et al., 1984) and HF (Patel and Zhang, 1996; Patel, 2000) and in the increase in sympathetic activity post MI. There is substantial evidence that the efficacy of the NO–GABA arm of the NTS–PVN circuit is reduced in these conditions (Zhang et al., 2002). However, this change may not be causal as recent evidence from our laboratory has shown that during the early stages of the progression to end stage HF, NO–GABA mediated inhibition is intact (Pyner et al., 2009). This would argue that progression to HF in the rat is a dynamic process, not initiated by removal or attenuation of NO–GABA interaction but associated with the maintenance of high sympathetic nerve activity in the later stages of the disease.

CONCLUSION

Neuroanatomical tract tracing combined with immunohistochemistry has identified glutamate neurons in the NTS that send axons to phenotypically specific populations of neurons in the PVN and its surrounds, including presympathetic neurons, GABA neurons, and nNOS-containing neurons. The organisation of the connections provides an anatomical explanation for the reflex action of the major cardiovascular receptors. Functionally, the neural circuits could underpin the regulation of sympathetic outflow and therefore have the potential to contribute to the generation of abnormal sympathetic activity by the PVN.

Acknowledgement—This work was funded by a British Heart Foundation project grant (PG/07/109/23994).

REFERENCES

Antunes VR, Yao ST, Pickering AE, Murphy D, Paton JF (2006) A spinal vasopressinergic mechanism mediates hyperosmolality-induced sympathoexcitation. J Physiol 576:569–583.

Benarroch E (2005) Paraventricular nucleus stress response and cardiovascular disease. Clin Auton Res 15:254–263.

Boudaba C, Szabo Z, Tasker JG (1996) Physiological mapping of local inhibitory inputs to the hypothalamic paraventricular nucleus. J Neurosci 16:7151–7160.

Ciriello J, Kline RL, Zhang TX, Caverson MM (1984) Lesions of the PVN alters the development of spontaneous hypertension in the rat. Brain Res 310:355–359.

Clement DL, Pelletier CL, Shepherd JT (1972) Role of vagal afferents in the control of renal sympathetic nerve activity in the rabbit. Circ Res 31:824–831.

Coote JH (2005) A role for the paraventricular nucleus of the hypothalamus in the autonomic control of heart and kidney. Exp Physiol 90:169–173.

Coote JH (2007) Landmarks in understanding the central nervous control of the cardiovascular system. Exp Physiol 92:3–18.

Dampney RAL (1994) Functional organisation of central pathways regulating the cardiovascular system. Physiol Rev 74:323–364.

Duale N, Waki H, Howorth P, Kasparov S, Teschmacher AG, Paton JF (2007) Restraining influence of A2 neurons in chronic control of arterial pressure in spontaneously hypertensive rats. Cardiovasc Res 76:184–193.

Feng D, Marshburn D, Jen DJ, Weinberg RJ, Taylor RM, Burette A (2007) Stepping into the third dimension. J Neurosci 27:12757–12760.

Floras JS (2009) Sympathetic nervous system activation in human heart failure. J Am Coll Cardiol 54:375–385.

Fuxe K, Dahlström AB, Jonsson G, Marcellino D, Guescini M, Dam M, Manger P, Agati L (2010) The discovery of central monoamine neurons gave volume transmission to the wired brain. Prog Neurobiol 90:82–100.

Goto A, Ikeda T, Tobian L, Iwai J, Johnson MA (1981) Brain lesions in the paraventricular nuclei and catecholaminergic neurons minimize salt hypertension in Dahl salt-sensitive rats. Clin Sci 61(Suppl. 7):53s–55s.

Grassi G, Seravalle G, Quarti-Trevano F, Dell'Oro R, Bolla G, Mancia G (2003) Effects of hypertension and obesity on the sympathetic activation of heart failure patients. Hypertension 42:873–877.

Hainsworth R (1991) Reflexes from the heart. Physiol Rev 71:617–658.

Haselton JR, Goering J, Patel KP (1994) Parvocellular neurons of the paraventricular nucleus are involved in the reduction in renal nerve discharge during isotonic volume expansion. J Auton Nerv Syst 50:1–11.

Herzog E, Bellenchi GC, Gras C, Bernard V, Ravassard P, Bedet C, Gasnier B, Giros B, El Mestikawy S (2001) The existence of a second vesicular glutamate transporter specifies subpopulations of glutamatergic neurons. J Neurosci Methods 21:RC181.

Henny P, Jones BE (2006) Innervation of orexin/hypocretin neurons by GABAergic, glutamatergic or cholinergic basal forebrain terminals evidenced by immunostaining for presynaptic vesicular transporter and postsynaptic scaffolding proteins. J Comp Neurol 499:645–661.

Hosoya Y, Sugiura Y, Okado N, Loewy AD, Kohno K (1991) Descending input from the hypothalamic paraventricular nucleus to sympathetic preganglionic neurons in the rat. Exp Brain Res 85:10–20.

Huang J, Weiss ML (1999) Characterisation of the central cell groups regulation the kidney in the rat. Brain Res 845:77–91.

Inokuchi H, Yoshimura M, Polosa C, Nishi S (1992) Adrenergic receptors (alpha 1 and alpha 2) modulate different potassium conductances in sympathetic preganglionic neruons. Can J Physiol Pharmacol 70:S92–S97.

Jan YN, Jan LY (1985) A LHRH-like peptidergic neurotransmitter capable of action at a distance in autonomic ganglia. In: Bousfield D, editor. Neurotransmitters in action. Amsterdam, New York, Oxford: Elsevier Biomedical Press. p. 94–103.

Jansen AS, Nguyen XV, Karpitskiy V, Mettenleiter TC, Loewy AD (1995) Central command neurons of the sympathetic nervous system: basis of the fight-or-flight response. Neuroscience 270:644–646.

Kannan H, Yamashita H (1988) Connections of neurons in the region of the nucleus tractus solitarius with the hypothalamic paraventricular nucleus: their possible involvement in neural control of the cardiovascular system in rat. Brain Res 329:205–212.

Kappagoda LT, Linden RJ, Snow HM (1973) Effect of stimulating right atrial receptors on urine flow in the dog. J Physiol 234:493–502.

Karim F, Kidd C, Malpus CM, Penna PC (1972) The effect of stimulation of the left atrial receptors on sympathetic efferent nerve activation. J Physiol 227:243–260.

Li D-P, Pan H-L (2006) Plasticity of GABAergic control of hypothalamic presympathetic neurons in hypertension. Am J Physiol 290:H1110–H1119.

Li D-P, Pan H-L (2007) Glutamatergic inputs in the hypothalamic paraventricular nucleus maintain sympathetic vasomotor tone in hypertension. Hypertension 49:916–925.

Li D-P, Chen S-R, Finnegan TF, Pan H-L (2004) Signaling pathway of nitric oxide in synaptic GABA release in the rat paraventricular nucleus. J Physiol 554:100–110.

Li YF, Roy SK, Channon KM, Zucker IH, Patel KP (2002) Effect of *in vivo* gene transfer of nNOS in the PVN on renal nerve discharge in rats. Am J Physiol 282:H594–H601.

Lin W, McKinney K, Liu L, Lakhlani S, Jennes L (2003) Distribution of vesicular glutamate transporter-2 messenger ribonucleic acid and protein in the septum–hypothalamus of the rat. Endocrinology 144:662–670.

Llewellyn-Smith IJ, Dicarlo SE, Collins HL, Keast JR (2005) Enkephalin-immunoreactive interneurons extensively innervate sympathetic preganglionic neurons regulating the pelvic viscera. J Comp Neurol 488:278–289.

Lovick TA, Coote JH (1988) Effects of volume loading on paraventriculo-spinal neurones in the rat. J Auton Nerv Syst 25:135–140.

Lovick TA, Coote JH (1989) Circulating atrial natriuretic factor activates vagal afferents inputs to paraventriculo-spinal neurones in the rat. J Auton Nerv Syst 26:129–134.

Lovick TA, Malpas SC, Mahoney M (1993) Renal vasodilatation in response to acute volume load is attenuated following lesions of parvocellular neurons in the paraventricular nucleus in rats. J Auton Nerv Syst 43:247–255.

Maley BE (1996) Immunohistochemical localisation of neuropeptides and neurotransmitters in the nucleus solitarius. Chem Senses 21:367–376.

McKellar S, Loewy AD (1981) Organisation of some brain stem afferents to the paraventricular hypothalamus in the rat. Brain Res 217:351–357.

Nylén A, Skagerberg G, Alm P, Larrsson B, Holmqvist BI, Anderson KE (2001) Detailed organisation of nitric oxide synthase, vasopressin and oxytocin immunoreactive cell bodies in the supraoptic nucleus of the female rat. Anat Embryol 203:309–407.

Patel KP (2000) Role of paraventricular nucleus in mediating sympathetic outflow in heart failure. Heart Fail Rev 5:73–86.

Patel KP, Zhang K (1996) Neurohumoral activation in heart failure: role of paraventricular nucleus. Clin Exp Pharmacol Physiol 23:722–726.

Paxinos G, Watson C (1998) The rat brain in stereotaxic coordinates. 4th ed. Academic Press.

Pilowsky P, Llewellyn-Smith IJ, Lipski J, Chalmers J (1992) Substance P immunoreactive boutons form synapses with feline sympathetic preganglionic neurones. J Comp Neurol 320:121–135.

Pyner S (2009) Neurochemistry of the paraventricular nucleus of the hypothalamus: implications for cardiovascular regulation. J Chem Neuroanat 38:197–208.

Pyner S, Coote JH (1999) Identification of an efferent projection from the paraventricular nucleus of the hypothalamus terminating close to spinally projecting rostral ventrolateral medullary neurons. Neuroscience 88:949–957.

Pyner S, Coote JH (2000) Identification of branching paraventricular neurons of the hypothalamus terminating close to spinally projecting rostral ventrolateral medullary neurons. Neuroscience 88:949–957.

Pyner S, Cleary J, McLeish P, Buchan A, Coote JH (2001) Tracing functionally identified neurons in a multisynaptic pathway in the hamster and rat using herpes simplex virus expressing green fluorescent protein. Exp Physiol 86:695–702.

Pyner S, Deering J, Coote JH (2002) Right atrial stretch induces renal nerve inhibition and c-fos expression in parvocellular neurons of the paraventricular nucleus in rats. Exp Physiol 87:25–32.

Pyner S, Pinkham MI, Guild SJ, Malpas SC, Whalley G, Barrett CJ (2009) Central brain nuclei and the development of sympathoexcitation after myocardial infarction. Proc Physiol Soc 15:PC81.

Reddy MK, Patel KP, Schultz HD (2007) Altered nitric oxide mechanism within the paraventricular nucleus contributes to the augmented carotid body chemoreflex in heart failure. Am J Physiol 292:H149–H157.

Reddy MK, Patel KP, Schultz HD (2005) Differential role of the paraventricular nucleus of the hypothalamus in modulating the sympathoexcitatory component of peripheral and central chemoreflexes. Am J Physiol 289:R789–R797.

Reiner A, Veenman CL, Medina L, Jiao Y, Del Mar N, Honig MG (2000) Pathway tracing using biotinylated dextran amines. J Neurosci Methods 103:23–37.

Ricardo J, Tongju K (1978) Anatomical evidence of direct projections from the nucleus of the solitary tract to the hypothalamus, amygdala and other forebrain structures in the rat. Brain Res 153:1–26.

Rumantir MS, Vaz M, Jennings GJ, Collier G, Kaye DM, Deals DR, Wiesner GH, Brunner-La Rocca HP, Esler MD (1999) Neural mechanisms in human obesity-related hypertension. J Hypertens 17:1125–1133.

Sawchenko PE, Swanson LW (1982) The organisation of noradrenergic pathways from the brainstem to the paraventricular and supraoptic nuclei in the rat. Brain Res 257:275–325.

Schramm LP, Strack AM, Platt KB, Loewy AD (1993) Peripheral and central pathways regulating the kidney: a study using pseudorabies virus. Brain Res 616:251–262.

Sobotka PA, Mahfoud F, Schlaich MO, Hoppe UC, Böhm M, Krum H (2011) Sympatho-renal axis in chronic disease. Clin Res Cardiol 100:1049–1057.

Spyer KM (1994) Central nervous mechanisms contributing to cardiovascular control. J Physiol 474(1):1–19.

Stern JE (2004) Nitric oxide and homeostatic control: an intracellular signalling molecule contributing to autonomic and neuroendocrine integration. Prog Biophys Mol Biol 84:197–215.

Strack AM, Sawyer WB, Hughes JH, Platt KB, Loewy AD (1989a) A general pattern of CNS innervation of the sympathetic outflow demonstrated by transneuronal pseudorabies viral infections. Brain Res 491:156–162.

Strack AM, Sawyer WB, Platt KB, Loewy AD (1989b) CNS cell groups regulating the sympathetic outflow to adrenal gland as revealed by transneuronal cell body labelling with pseudorabies virus. Brain Res 491:274–296.

Swanson LW, Sawchenko PE (1983) Hypothalamic integration: organisation of the paraventricular and supraoptic nuclei. Annu Rev Neurosci 6:269–324.

Ter Horst Gj, De Boer P, Luiten PGM, van Willigen JD (1989) Ascending projections from the solitary tract nucleus to the hypothalamus. A *Phaseolus vulgaris* lectin tracing study in the rat. Neuroscience 31:785–797.

Ulrich-Lai YM, Jones KR, Ziegler DR, Cullinan WE, Herman JP (2011) Forebrain origins of glutamatergic innervation to the rat paraventricular nucleus of the hypothalamus: differential inputs to the anterior versus posterior subregions. J Comp Neurol 519:1301–1319.

Watkins ND, Cork SC, Pyner S (2009) An immunohistochemical investigation of the relationship between NOS, GABA and pre-sympathetic paraventricular neurons in the hypothalamus. Neuroscience 159:1079–1088.

Wouterlood FG, van Haeften T, Blijleven N, Perez-Templado P, Perez-Templado E (2002) Double labelled confocal laser-scanning microscopy, image restoration, and real-time three-dimensional reconstruction to study axons in the central nervous system and their contacts with target neurons. Appl Immunohistochem Mol Morphol 10:85–95.

Wouterlood FG, Böckers T, Witter MP (2003) Synaptic contacts between identified neurons visualised in the confocal laser-scanning microscope. Neuroanatomical tracing combined with immunofluorescence detection of post-synaptic density proteins and target neuron-markers. J Neurosci Meths 128:129–142.

Yang Z, Coote JH (2003) Role of GABA and NO in the paraventricular nucleus-mediated reflex inhibition of renal sympathetic nerve activity following stimulation of right atrial receptors in the rat. Exp Physiol 88:335–342.

Yang Z, Coote JH (2006) The role of supraspinal vasopressin and glutamate neurones in an increase in renal sympathetic activity in response to mild haemorrhage in the rat. Exp Physiol 91:791–797.

Zhang K, Mayhan WG, Patel KP (1997) Nitric oxide within the paraventricular nucleus mediates changes in renal sympathetic nerve activity. Am J Physiol 273:R864–R872.

Zhang K, Li YF, Patel KP (2002) Reduced endogenous GABA-mediated inhibition in the PVN on renal nerve discharge in rats with heart failure. Am J Physiol 282:R864–R872.

Zhang ZH, Yu Y, Kang YM, Wei SG, Felder RB (2008) Aldosterone acts centrally to increase brain renin–angiotensin system activity and oxidative stress in normal rats. Am J Physiol 294:H1067–H1074.

Ziegler DR, Edwards MR, Ulrich-Lai YM, Herman JP, Cullinan E (2012) Brainstem origins of glutamatergic innervation of the rat hypothalamic paraventricular nucleus. J Comp Neurol. http://dx.doi.org/10.1002/cne.23043.

(Accepted 7 May 2012)
(Available online 12 June 2012)